Chapter 10
Phase Transformations in Calcium Phosphate Crystallization

Henrik Birkedal

10.1 Introduction

The crystallization of calcium phosphates has fascinated researchers for many decades, especially because of the role of apatites in the biomineralization of bone and teeth but also due to its relevance for geochemistry (Hughes and Rakovan 2015). There is an enormous body of work on calcium phosphates in the literature (Wang and Nancollas 2008; Dorozhkin 2009; Elliott 1994). Several calcium phosphates can be obtained from precipitation experiments, including hydroxyapatite ($Ca_{10}(PO_4)_6(OH)_2$, HAP), octacalcium phosphate ($Ca_8H_2(PO_4)_6 \cdot 5(H_2O)$, OCP), brushite ($CaHPO_4 \cdot 2(H_2O)$), and monetite ($CaHPO_4$). Herein, we will mostly cover aspects related to the mechanisms of crystallization and almost exclusively focus on pathways leading to apatite formation.

Crystallization research has undergone a renaissance over the last decade or two. While attempts have been made to establish a unifying picture of inorganic crystallization processes based on the numerous recent findings (De Yoreo et al. 2015; De Yoreo et al. 2017, Chap. 1), many important fundamental questions remain unanswered, particularly in systems like the calcium phosphates. These questions pertain both to idealized laboratory conditions (Delgado-Lopez and Guagliardi 2017, Chap. 11) and to the formation of biogenic calcium phosphate minerals in vivo (Falini and Fermani 2017, Chap. 9). In the latter context, several new perspectives have emerged recently, including the idea that citrate ions constitute an integral part of nanoparticle aggregates in bone, forming organic bridges between minute inorganic crystals (Davies et al. 2014).

H. Birkedal (✉)
Department of Chemistry and iNANO, Aarhus University, Gustav Wieds Vej 14, 8000 Aarhus, Denmark
e-mail: hbirkedal@chem.au.dk

A.E.S. Van Driessche et al. (eds.), *New Perspectives on Mineral Nucleation and Growth*,
DOI 10.1007/978-3-319-45669-0_10

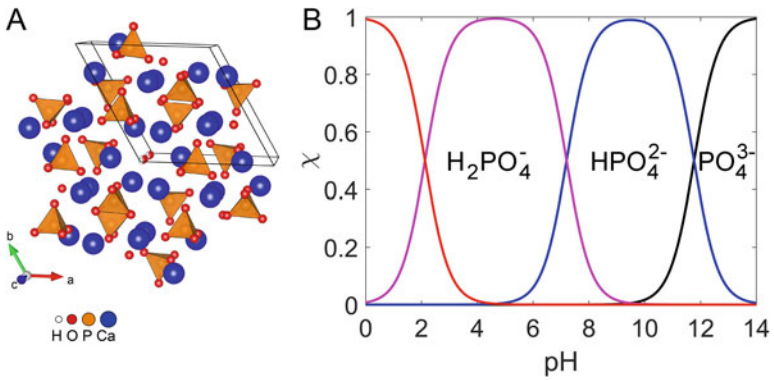

Fig. 10.1 (**a**) Hexagonal apatite crystal structure with disordered hydroxyl ion orientations. (**b**) pH dependence of the speciation of phosphate in aqueous solution

Hydroxyapatite (HAP) has an ideal composition of $Ca_{10}(PO_4)_6(OH)_2$. However, there is a wide range of possible substitutions; for example, carbonate ions can substitute on either the phosphate or hydroxide position (Fig. 10.1a), with the former occurring almost exclusively at low temperature and in biogenic apatites. HAP is typically hexagonal with disordered hydroxide ion orientations, as shown in Fig. 10.1a. The ordered monoclinic form is usually not observed in apatite obtained from syntheses giving nanocrystals.

In aqueous solution, phosphate speciation is strongly dependent on pH as shown in Fig. 10.1b. This means that the free phosphate concentration at pH values below about 9 is negligible. It should be recalled, however, that coordination to metal ions such as calcium changes the effective acidity constant and can strongly influence acid/base equilibria.

In the following, various aspects of calcium phosphate formation will be discussed, starting with a brief account of amorphous calcium phosphates (ACPs) and progressing via prenucleation phenomena to a presentation of recent results from our laboratory on the crystallization of HAP from ACP, to end with a recapitulation of current works on the importance of confinement for calcium phosphate crystallization.

10.2 Amorphous Calcium Phosphates

Amorphous calcium phosphate forms easily from aqueous solution, where it subsequently transforms into, e.g., HAP. There are several excellent reviews on this subject (Combes and Rey 2010; Dorozhkin 2010) and the present discussion will therefore be kept brief. Today it is clear that there are many ways to stabilize ACPs, for example, by the addition of organic additives or foreign ions such as carbonate or pyrophosphate. However, the “true” structure of ACPs is still a matter of debate.

Posner and Betts used X-ray diffraction to derive a structural model for the basic building block of ACP in the form typically obtained under basic conditions (Posner and Betts 1975). Through pair-distribution function (PDF) analysis, they proposed that ACP is built from $Ca_9(PO_4)_6$ clusters that are interspersed with water to form the larger spheroids observed experimentally in electron microscopy. These so-called Posner clusters have been central to most discussions about ACP and apatite crystallization ever since. Meanwhile it is known that there are several different structural forms of ACP (Combes and Rey 2010; Dorozhkin 2010), depending on the way in which they are prepared – much like in the case of calcium carbonate (Fernandez-Martinez et al. 2017, Chap. 4, this volume). It is also clear that while Posner clusters certainly explain part of the phenomena observed, they are not able to account for all features observed for ACPs. Thus there is an urgent need for improved models of the structure and composition of ACPs, especially because their importance as precursor species in HAP and biogenic apatite formation increases, as discussed below and elsewhere in this book (Delgado-Lopez and Guagliardi 2017, Chap. 11, this volume). Recent improvements in PDF analysis methods, including the ability to perform in situ experiments, promise deeper insights into the structure of ACPs (Tyrsted et al. 2014), especially when combined with advanced NMR (Davies et al. 2014) and TEM (Dey et al. 2010; Nudelman et al. 2010; Nielsen and De Yoreo 2017, Chap. 18) techniques.

10.3 Prenucleation Phenomena

At concentrations below saturation, ion pairs have been known to form for a long time (Berry et al. 2000). In 2008, however, it was suggested that somewhat larger clusters, termed prenucleation clusters, occur in the $CaCO_3$ system (Gebauer et al. 2008; Gebauer et al. 2014). They have also been reported for silica (Tobler et al. 2017, Chap. 15) and iron oxyhydroxide (Reichel and Faivre 2017, Chap. 12 and Penn et al. 2017, Chap. 13) and some other systems (Gebauer et al. 2014). In solutions of zirconium acetate, from which zirconia forms upon heating, metastable polymeric states were observed (Bremholm et al. 2015) and have been shown to be directly involved in crystallization through a series of structural rearrangements (Tyrsted et al. 2014).

For calcium phosphates, there were early suggestions by Posner and Betts that such clusters should exist in solution, even though this was based exclusively on indirect evidence from their work on solid ACP (Posner and Betts 1975). Using light scattering and other techniques, Onuma and Ito (1998) detected calcium phosphate clusters in simulated body fluid (SBF) at pH 7.4, but also in acidified SBF solutions at pH 5.3, which are only supersaturated with respect to HAP but undersaturated with respect to octacalcium phosphate and ACP. These clusters were 0.7–1.1 nm in diameter, consistent with the size of Posner clusters. Moreover, the authors suggested a cluster aggregation model for crystal growth of HAP. More recently, Dey et al. (2010) used cryo-TEM to study the early stages of the formation of apatite

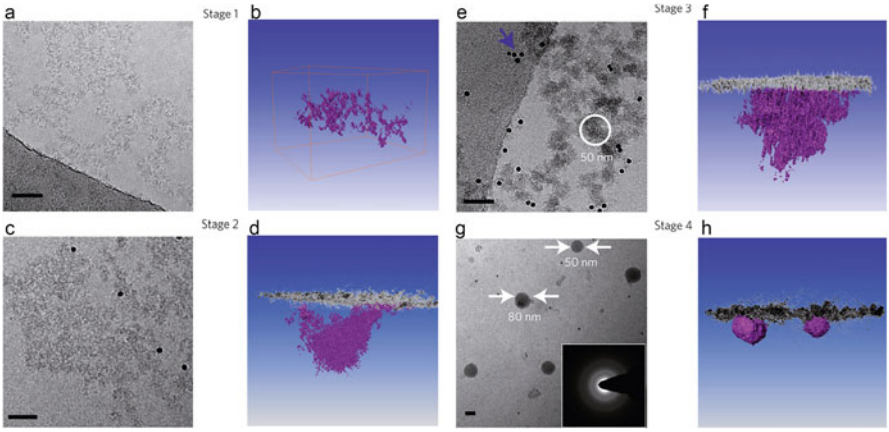

Fig. 10.2 Cryo-TEM studies of prenucleation clusters and the early stages of ACP formation from SBF solution in contact with a monolayer of arachidic acid. Panels *a*, *c*, *e*, and *g* are 2D projected TEM images with scale bars of 50 nm. Panels *b*, *d*, *f*, and h are corresponding 3D computer renderings of cryo-TEM tomograms with the monolayer shown in *gray* and the calcium phosphate in *purple*. The inset in panel *g* is a selected-area electron diffraction image showing that the particles are amorphous. Adapted and reprinted with permission from Macmillan Publishers Ltd: Nature Materials (Dey et al. 2010), copyright 2010

from SBF at 37 °C at the surface of a Langmuir monolayer of arachidic acid in a "frozen-snapshot" manner, where selected stages of the growth process could be resolved by stabilizing them through vitrification. Clusters were observed in solution also in this study, as shown in Fig. 10.2a, b. Their sizes were consistent with those of Posner clusters, although their chemical composition again remained undetermined. Upon contact with the arachidic acid monolayer, the clusters accumulated at the interface forming fractal aggregates (Fig 10.2c, d), which condensed further over time (Fig. 10.2e, f) to form dense ACP globules (Fig. 10.2g, h), shown to be amorphous by electron diffraction (inset of Fig. 10.2g), that ultimately crystallized to yield HAP. It should be stressed that the identification of the observed nanometric species as Posner clusters is based mostly on size. Secondly, in both works cited above, the investigated solutions were supersaturated with respect to HAP. Thus these clusters are not necessarily prenucleation clusters per se (Gebauer et al. 2014), but rather they should be considered as strong indications that prenucleation phenomena are also at play in calcium phosphate systems.

In another recent study, Habraken et al. (2013) conducted experiments where TRIS buffer solutions of calcium and phosphate salts were mixed at an initial pH of 7.4 and a Ca:P molar ratio of 1.43. Subsequently, the authors followed the progress of the reaction by ion-selective electrodes and pH measurements. Based on the data, a model was proposed in which the initially formed clusters are assumed to be highly charged with the composition $[Ca(HPO_4)_3]^{4-}$, while 57 % of these species are protonated ($[Ca(HPO_4)_2(H_2PO_4)]^{3-}$) under the given conditions. With time, these charged complexes were suggested to take up a calcium ion, and the

resulting clusters (i.e., $[Ca_2(HPO_4)_3]^{2-}$) would then form the basis of ACP by building up a fractal network. This speciation model has been criticized in particular due to the fact that it is based on ion association constants from the literature, which were obtained without accounting for cluster formation, and by the question of how such highly charged ion complexes would aggregate without an additional charge-compensating step (Gebauer et al. 2014). Again the work of Habraken et al. took place under supersaturated conditions with respect to all crystalline phases.

Thus there are strong – almost "smoking gun" – indications that prenucleation clusters may occur in the calcium phosphate system, but still complete and conclusive evidence in particular for undersaturated conditions is missing. In addition, most studies were performed at pH levels very close to 7.4, even though HAP is known to form much more readily at high pH. This choice has presumably been based on the use of SBF as a biologically relevant fluid. However, in actual body fluid, crystallization is suppressed by a range of mechanisms to avoid mineralization, and hence one is left to wonder how particularly biologically relevant these conditions are (see also below).

10.4 Crystallization of HAP

The formation of HAP crystals demands either a transformation from preformed ACP or the agglomeration/association of prenucleation clusters and/or ions. Which particular pathway is followed must depend on several factors, including concentration and pH (Delgado-Lopez and Guagliardi 2017, Chap. 11).

To understand the crystallization process, it is essential to be able to study it as it happens, i.e., using in situ techniques. The amorphous phase is supposed to have spherical morphology, whereas apatite crystals are strongly anisotropic in shape. From the hexagonal symmetry, a needlelike morphology can be expected, which is indeed observed in synthetic and geological apatites (Hughes and Rakovan 2015). In teeth, the crystals are needle-shaped, while in bone, they are predominantly nanoplates (Mann 2001; Weiner and Wagner 1998). However, it has been an open question at what point during crystal growth the anisotropic morphology is attained, i.e., when one transitions from a sphere to an anisotropic shape. This question is related to the crystal surface energy, and thus it is tightly connected to phase stability and its dependence on nanocrystal size (Jensen et al. 2010). One suitable technique for studying crystallization kinetics is to use synchrotron in situ X-ray diffraction. This allows quantifying how much crystalline material is formed over time, but it can also yield the lattice constants of the forming crystals and, by analysis of the diffraction peak widths, the nanocrystal shape. We have reported several such studies based on a custom-designed stopped-flow apparatus (Ibsen and Birkedal 2010; Ibsen and Birkedal 2012; Jensen et al. 2015; Ibsen et al. 2016a; Ibsen et al. 2016b). We mixed calcium- and phosphate-containing solutions to induce the formation of ACP under the desired temperature and pH conditions. The ACP phase

was formed directly in the X-ray diffraction cell, thus allowing its crystallization to be monitored in situ with excellent time resolution. We precipitated ACP both with (Ibsen and Birkedal 2010; Ibsen and Birkedal 2012) and without additives (Ibsen et al. 2016a; Ibsen et al. 2016b); herein we shall only discuss the latter case. Apatite was obtained by the following reaction sequence:

$$10CaCl_2 + 6M_3PO_4 + xMOH \rightarrow ACP \rightarrow HAP \tag{10.1}$$

where M^+ is either Na^+ or K^+ and the initial calcium concentration was 0.2 M, with x equaling either 2 or 0 to correspond to stoichiometric HAP ($x = 2$) or HPO_4^{2-}-dominated conditions.

Due to the extensive substitution chemistry of apatites, it is essential to carefully consider which counterions to use. With sodium as phosphate counterion, carbonate (from dissolved atmospheric CO_2) can substitute into the apatite lattice, while with potassium this does not happen as evidenced by FTIR spectroscopy (Ibsen et al. 2016b). For $x = 2$ in reaction (1), the initial solution is dominated by phosphate, while with $x = 0$, HPO_4^{2-} is the main phosphate species (cf. Fig. 10.1b). In the phosphate-dominated case, the crystals had a small aspect ratio at early stages, suggesting that the initial nuclei were close to spherical in shape. They then rapidly grew along the *c*-axis and only much slower in the (*a*,*b)* plane, resulting in anisotropic particles. The nanocrystal size and formation kinetics depended on the choice of the counterion, i.e., sodium or potassium (Ibsen et al. 2016b), with potassium yielding more slender and longer needles than sodium.

Under HPO_4^{2-}-dominated conditions and with potassium as counterion, the observed crystallization behavior was very different than in the phosphate-dominated case discussed above. Figure 10.3 displays some of the kinetic data obtained at 60 °C, which we will discuss in some more detail here to illustrate the large degree of information that can be obtained by high-quality in situ diffraction methods (Ibsen et al. 2016a). The raw diffraction data show strong scattering signal of the aqueous solvent (Fig. 10.3a), but it was nevertheless possible to extract high-quality diffraction data by subtracting the solvent scattering (Fig. 10.3b). Initially, only the scattering signal of ACP was observed as two broad diffuse maxima at $2\theta \approx 12°$ and 18°. After a while, diffraction peaks from HAP appeared, while no other crystalline phases could be observed. The data were treated by Rietveld refinement. The Rietveld scale factor is a measure of the amount of crystalline material present. As seen in Fig. 10.3c, it increased rapidly to a plateau after a short induction time and remained constant thereafter, showing that the amount of crystalline material did not change after this nucleation burst. The nanocrystal size and composition, however, evolved over longer periods of time. In stark contrast to the phosphate-dominated situation, the initially detected nanocrystals were highly anisotropic, only ~3.5 nm wide, and almost ten times longer, as shown in Fig. 10.3e, 10.3f. The shape aspect ratio decreased in two stages, a rapid initial drop followed by a slower decay (Fig. 10.3e). During the early stage of growth, the chemistry of the crystals changes drastically. Initially, they were found to be highly Ca deficient as shown in Figure 10.3d, where the Ca occupation in the HAP unit cell is plotted as a

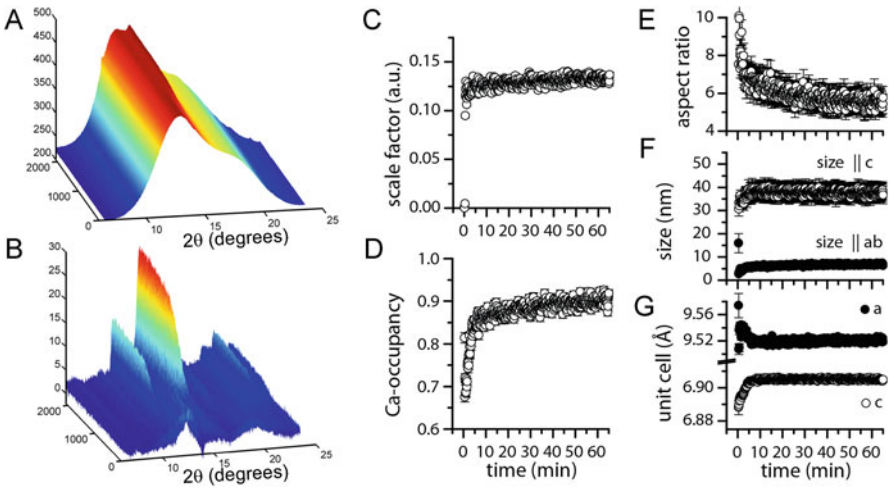

Fig. 10.3 In situ X-ray diffraction data on apatite nanocrystal formation under HPO_4^{2-}-dominated conditions (for explanations see text). Adapted from (Ibsen et al. 2016a) with permission from the publisher

function of time. There is first a rapid increase in the average calcium content of the nanocrystals followed by a stage of slower Ca uptake.

This behavior is also reflected in the time evolution of the unit cell parameters shown in Fig. 10.3g and was interpreted as follows: the initial Ca deficiency is most likely charge-compensated by hydrogen phosphate resulting in compositions of the general formula $Ca_{10-y}(HPO_4)_{2y}(PO_4)_{6-2y}(OH)_2$. The initial highly anisotropic nanocrystals had a composition close to $y = 3$, i.e., with all phosphates being hydrogenated. At later stages of growth, y approached 1. In a simple model, we assumed that stoichiometric HAP was added to a fully hydrogenated initial nanocrystal; this allowed predicting the Ca occupancy with the nanocrystal volumes as obtained from their measured sizes (Fig. 10.3f). A nearly perfect match to the experimentally determined time evolution of the Ca occupancy was found (Ibsen et al. 2016a). The presence of HPO_4^{2-} was confirmed by FTIR, an example of which is shown in Fig. 10.4. As expected with potassium as counterion, no carbonate peaks are observed, but a clear hydrogen phosphate resonance occurs at ca. 871 cm^{-1}.

OCP has long been suggested to be a precursor phase in biological apatite formation (Brown and Chow 1976), and more recent Raman spectroscopic studies of in vitro mineralization experiments point in the same direction (Crane et al. 2006). However, other evidence indicates that ACP is the relevant precursor material in biogenic crystallization, as first shown in chiton teeth (Lowenstam and Weiner 1985) and more recently in the youngest tissue of continuously forming special bones of zebrafish fin rays (Mahamid et al. 2010) as well as in more common bone (Mahamid et al. 2011). There has thus been a controversy about whether the initial phase is indeed ACP/OCP or ACP/nonstoichiometric apatite crystals (Weiner 2006; Grynpas 2007).

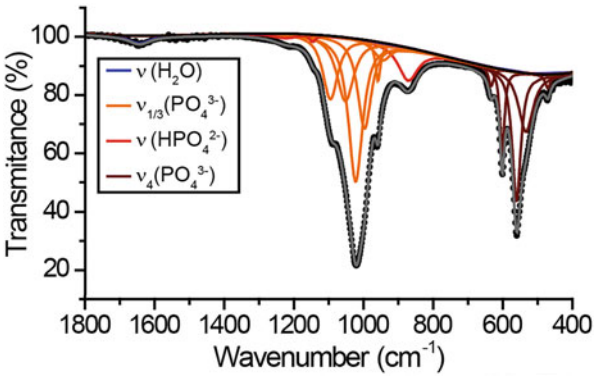

Fig. 10.4 FTIR spectrum of HAP nanocrystals obtained under HPO_4^{2-}-dominated conditions with potassium as counterion (Adapted from (Ibsen et al. 2016a) with permission from the publisher)

10.5 Confinement Effects

It has become clear that the physical environment plays a key role in deciding how crystallization proceeds, as documented in particular for the case of biogenic apatite formation (Weiner and Wagner 1998; Mann 2001; Olszta et al. 2007; Gower 2008). Rajasekharan and Andersson, for example, have recently reported the formation of crystalline calcium phosphates from amorphous calcium phosphate within the pores of polymerized liquid crystals and found that the pore size of aqueous domains influenced the outcome of crystallization (Rajasekharan and Andersson 2015). Polymerized liquid crystals were obtained by using functionalized Pluronic F127 ($EO_{100}PO_{70}EO_{100}$, where EO is ethylene oxide and PO is propylene oxide), which was crystallized into a hexagonal mesoporous material and then polymerized to yield covalently cross-linked mesoporous networks with excellent mechanical stability (He et al. 2015). These structures were infiltrated with acidic calcium and phosphate solutions at high concentrations. Subsequent exposure to ammonia gas triggered crystallization through a pH increase, leading to ACP formation in the pores of the mesoporous scaffold. With pore sizes below ~10 nm, nanocrystalline HAP was obtained, while a mixture of acidic polymorphs (monetite and brushite) were formed at larger pore sizes (Rajasekharan and Andersson 2015). This method gave purely artificial materials reminiscent of bone (He et al. 2015). Interestingly, confinement can also stabilize ACP and influence the alignment and morphology of the resulting crystals, as shown by Cantaert et al. (2013) using anodized alumina membranes. Likewise, growth of calcium phosphates on patterned, carboxylate-functionalized substrates with gelatin as growth modifier results in ultrahigh aspect ratio nanocrystals oriented perpendicular to the substrate (Tseng et al. 2013). It has also been proven possible to form apatites as chemical gardens using metal-loaded gelatin gels as metal reservoirs (Ibsen et al. 2014). All these findings illustrate how both physical and chemical factors can influence calcium phosphate mineralization.

10.6 Outlook

While great strides have been made in the understanding of calcium phosphate mineralization in general and ACP and HAP formation in particular, a range of open questions remain that need to be addressed in the coming years. As has been argued throughout this chapter, the strong pH dependence of phosphate speciation suggests that there is not one universal mechanism of calcium phosphate mineralization.

The nature of ACP remains a mystery and there is a strong need for improved structural models of ACPs formed under various conditions. With recent developments in, e.g., pair-distribution function analysis and NMR, it seems likely that this goal will be attained within a few years.

The prenucleation state and the steps leading to ACP formation remain contested, and much more work is needed before this part of the calcium phosphate picture is painted. This problem is challenging for several reasons. First and foremost, there is a technical challenge: the low solubility of HAP means that solutions undersaturated with respect to HAP have very low concentrations of the relevant species, which renders the range of applicable experimental techniques limited. Secondly, there is a need for establishing widely accepted methodologies for detecting these phenomena. In the view of the present author, the titration approach employed by Gebauer et al. (2008) is promising, even though it also suffers from drawbacks including a varying ionic strength. The next challenge is to identify which species are present in any detected clusters. As argued above, phosphate speciation changes drastically with pH. Even when taking into account the possible change in effective pK_a due to coordination by, e.g., calcium, there is likely to be several types of cluster compositions that will change with pH. The situation is further complicated by the ability of phosphate to undergo self-oligomerization through condensation, leading to pyrophosphate and higher polyphosphates that are both potent inhibitors of crystallization (Omelon and Grynpas 2008; Omelon et al. 2013) and species that must be considered for a full description of solution composition. These challenges call for novel and above all systematic approaches employing several complementary techniques, both experimental and theoretical.

The crystallization process itself also deserves more attention. An exceedingly large number of additives that affect calcium phosphate crystallization have been identified. Many of these are of relevance to biomineralization, even though it remains unclear which species are the main actors in which type of biomineralization. As shown in this chapter, the crystallization kinetics are very diverse and studying them with in situ techniques provides extremely valuable information, which ultimately can afford very detailed insights into crystallization pathways and (with additional model input) shed light on the relative importance of terms contributing to surface energies (Jensen et al. 2010). Above all there is a need for systematic studies including variations of the Ca:P ratio, pH, temperature, and solution composition. This will pave the way for understanding the factors determining, e.g., nanocrystal morphology evolution.

Thus, while much has been learned about calcium phosphate crystallization in the past years, we have only scratched the surface to reveal that much more is yet to be understood.

References

Anderson HC, Garimella R, Tague SE (2005) The role of matrix vesicles in growth plate development and biomineralization. Front Biosci 10:822–837

Berry RS, Rice SA, Ross J (2000) Physical chemistry. Oxford University Press, Oxford

Boonrungsiman S, Gentleman E, Carzaniga R, Evans ND, Mccomb DW, Porter AE, Stevens MD (2012) The role of intracellular calcium phosphate in osteoblast-mediated apatite formation. Proc Natl Acad Sci U S A 109:14170–14175

Bremholm M, Birkedal H, Iversen BB, Pedersen JS (2015) Structural evolution of aqueous zirconium acetate by time-resolved small-angle X-ray scattering and rheology. J Phys Chem C 119:12660–12667

Brown WE, Chow LC (1976) Chemical properties of bone-mineral. Annu Rev Mater Sci 6:213–236

Cantaert B, Beniash E, Meldrum FC (2013) Nanoscale confinement controls the crystallization of calcium phosphate: relevance to bone formation. Chem Eur J 19:14918–14924

Combes C, Rey C (2010) Amorphous calcium phosphates: synthesis, properties and uses in biomaterials. Acta Biomater 6:3362–3378

Crane NJ, Popescu V, Morris MD, Steenhuis P, Ignelzi MA (2006) Raman spectroscopic evidence for octacalcium phosphate and other transient mineral species deposited during intramembranous mineralization. Bone 39:434–442

Davies E, Müller KH, Wong WC, Pickard CJ, Reid DG, Skepper JN, Duer MJ (2014) Citrate bridges between mineral platelets in bone. Proc Natl Acad Sci U S A 111:E1354–E1363

De Yoreo JJ, Gilbert PUPA, Sommerdijk NAJM, Penn RL, Whitelam S, Joester D, Zhang H, Rimer JD, Navrotsky A, Banfield JF, Wallace AF, Michel FM, Meldrum FC, Cölfen H, Dove PM (2015) Crystallization by particle attachment in synthetic, biogenic, and geologic environments. Science 349(498):aaa6760-1–aaa6760-9

De Yoreo JJ, Sommerdijk NAJM, Dove PM (2017) Nucleation pathways in electrolyte solutions. In: Van Driessche AES, Kellermeier M, Benning LG, Gebauer D (eds) New perspectives on mineral nucleation and growth, Springer, Cham, pp 1–24

Delgado-López JM, Guagliardi A (2017) Control over nanocrystalline apatite formation: what can the X-ray total scattering approach tell us. In: Van Driessche AES, Kellermeier M, Benning LG, Gebauer D (eds) New perspectives on mineral nucleation and growth, Springer, Cham, pp 211–226

Dey A, Bomans PHH, Müller FA, Will J, Frederik PM, De With G, Sommerdijk NAJM (2010) The role of prenucleation clusters in surface-induced calcium phosphate crystallization. Nat Mater 9:1010–1014

Dorozhkin SV (2009) Calcium orthophosphates in nature. Biol Med Mater 2:399–498

Dorozhkin SV (2010) Amorphous calcium (ortho)phosphates. Acta Biomater 6:4457–4475

Elliott JC (1994) Structure and chemistry of the apatite and other calcium orthophosphates. Elsevier, Amsterdam

Falini G, Fermani S (2017) Nucleation and growth from a biomineralization perspective. In: Van Driessche AES, Kellermeier M, Benning LG, Gebauer D (eds) New perspectives on mineral nucleation and growth, Springer, Cham, pp 185–198

Fernandez-Martinez A, Lopez-Martinez H, Wang D (2017) Structural characteristics and the occurrence of polyamorphism in amorphous calcium carbonate. In: Van Driessche AES, Kellermeier M, Benning LG, Gebauer D (eds) New perspectives on mineral nucleation and growth, Springer, Cham, pp 77–92

Gebauer D, Völkel A, Cölfen H (2008) Stable prenucleation calcium carbonate clusters. Science 322:1819–1822

Gebauer D, Kellermeier M, Gale JD, Bergström L, Cölfen H (2014) Pre-nucleation clusters as solute precursors in crystallisation. Chem Soc Rev 43:2348–2371

Gower LB (2008) Biomimetic model systems for investigating the amorphous precursor pathway and its role in biomineralization. Chem Rev 108:4551–4627

Grynpas MD (2007) Transient precursor strategy or very small biological apatite crystals? Bone 41:162–164

Habraken WJEM, Tao J, Brylka LJ, Friedrich H, Bertinetti L, Schenk AS, Verch A, Dmitrovic V, Bomans PHH, Frederik PM, Laven J, Van der Schoot P, Aichmayer B, De With G, Deyoreo JJ, Sommerdijk NAJM (2013) Ion-association complexes unite classical and non-classical theories for the biomimetic nucleation of calcium phosphate. Nat Commun 4:1507

He W-X, Rajasekharan AN, Tehrani-Bagha AR, Andersson M (2015) Mesoscopically ordered bone-mimetic nanocomposites. Adv Mater 27:2260–2264

Hu Y-Y, Rawal A, Schmidt-Rohr K (2010) Strongly bound citrate stabilizes the apatite nanocrystals in bone. Proc Natl Acad Sci U S A 107:22425–22429

Hughes JM, Rakovan JF (2015) Structurally robust, chemically diverse: apatite and apatite supergroup minerals. Elements 11:165–170

Ibsen CJS, Birkedal H (2010) Modification of bone-like apatite nanoparticle size and growth kinetics by alizarin red S. Nanoscale 2:2478–2486

Ibsen CJS, Birkedal H (2012) Influence of poly(acrylic acid) on apatite formation studied by in situ X-ray diffraction using an X-ray scattering reaction cell with high-precision temperature control. J Appl Crystallogr 45:976–981

Ibsen CJS, Mikladal BF, Jensen UB, Birkedal H (2014) Hierarchical tubular structures grown from the gel/liquid interface. Chem Eur J 20:16112–16120

Ibsen CJS, Chernyshov D, Birkedal H (2016a) Apatite formation from amorphous calcium phosphate and mixed amorphous calcium phosphate/amorphous calcium carbonate. Chem Eur J 22:12347–12357

Ibsen CJS, Leemreize H, Mikladal BF, Skovgaard J, Eltzholtz JR, Bremholm M, Iversen BB, Birkedal H (2016b) Crystallization kinetics of bone-like apatite nanocrystals formed from amorphous calcium phosphate in water by in situ synchrotron powder diffraction: counter ions matter (Submitted)

Jensen GV, Bremholm M, Lock N, Deen GR, Jensen TR, Iversen BB, Niederberger M, Pedersen JS, Birkedal H (2010) Anisotropic crystal growth kinetics of anatase TiO2 nanoparticles synthesized in a nonaqueous medium. Chem Mater 22:6044–6055

Jensen ACS, Hinge M, Birkedal H (2015) Calcite nucleation on the surface of PNIPAM-PAAc micelles studied by time resolved *in situ* PXRD. CrystEngComm 17:6940–6946

Lowenstam HA, Weiner S (1985) Transformation of amorphous calcium-phosphate to crystalline dahllite in the radular teeth of chitons. Science 227:51–53

Mahamid J, Aichmayer B, Shimoni E, Ziblat R, Li C, Siegel S, Paris O, Fratzl P, Weiner S, Addadi L (2010) Mapping amorphous calcium phosphate transformation into crystalline mineral from the cell to the bone in zebrafish fin rays. Proc Natl Acad Sci U S A 107:6316–21

Mahamid J, Sharir A, Gur D, Zelzer E, Addadi L, Weiner S (2011) Bone mineralization proceeds through intracellular calcium phosphate loaded vesicles: a cryo-electron microscopy study. J Struct Biol 174:527–535

Mann S (2001) Biomineralization: principles and concepts in bioinorganic materials chemistry. Oxford University Press, Oxford

Nielsen MH, De Yoreo JJ (2017) Liquid phase TEM investigations of crystal nucleation, growth, and transformation. In: Van Driessche AES, Kellermeier M, Benning LG, Gebauer D (eds) New perspectives on mineral nucleation and growth, Springer, Cham, pp 353–371

Nudelman F, Pieterse K, George A, Bomans PHH, Friedrich H, Brylka LJ, Hilbers PAJ, De With G, Sommerdijk NAJM (2010) The role of collagen in bone apatite formation in the presence of hydroxyapatite nucleation inhibitors. Nat Mater 9:1004–1009

Olszta MJ, Cheng X, Jee SS, Kumar R, Kim Y-Y, Kaufman MJ, Douglas EP, Gower LB (2007) Bone structure and formation: a new perspective. Mater Sci Eng R 58:77–116

Omelon S, Grynpas MD (2008) Relationships between polyphosphate chemistry, biochemistry and apatite biomineralization. Chem Rev 108:4694–4715

Omelon S, Ariganello M, Bonnucci E, Grynpas M, Nanci A (2013) A review of phosphate mineral nucleation in biology and geobiology. Calcif Tissue Int 93:382–396

Onuma K, Ito A (1998) Cluster growth model for hydroxyapatite. Chem Mater 10:3346–3351

Posner AS, Betts F (1975) Synthetic amorphous calcium phosphate and its relation to bone mineral structure. Acc Chem Res 8:273–281

Penn RL, Li D, Soltis JA (2017) A perspective on the particle-based crystal growth of ferric oxides, oxyhydroxides, and hydrous oxides. In: Van Driessche AES, Kellermeier M, Benning LG, Gebauer D (eds) New perspectives on mineral nucleation and growth, Springer, Cham, pp 257–274

Rajasekharan AN, Andersson M (2015) Role of nanoscale confinement on calcium phosphate formation at high supersaturation. Cryst Growth Des 15:2775–2780

Reichel V, Faivre D (2017) Magnetite nucleation and growth. In: Van Driessche AES, Kellermeier M, Benning LG, Gebauer D (eds) New perspectives on mineral nucleation and growth, Springer, Cham, pp 275–292

Tobler DJ, Stawski TM, and Benning LG (2017) Silica and alumina nanophases: natural processes and industrial applications. In: Van Driessche AES, Kellermeier M, Benning LG, Gebauer D (eds) New perspectives on mineral nucleation and growth, Springer, Cham, pp 293–316

Tseng Y-H, Birkbak ME, Birkedal H (2013) Spatial organization of hydroxyapatite nanorods on a substrate via a biomimetic approach. Cryst Growth Des 13:4213–4219

Tyrsted C, Lock N, Jensen KMØ, Christensen M, Bøjesen ED, Emerich H, Vaughan G, Billinge SJL, Iversen BB (2014) Evolution of atomic structure during nanoparticle formation. IUCrJ 1:165–171

Wang L, Nancollas GH (2008) Calcium orthophosphates: crystallization and dissolution. Chem Rev 108:4628–4669

Weiner S (2006) Transient precursor strategy in mineral formation of bone. Bone 39:431–433

Weiner S, Wagner HD (1998) The material bone: structure-mechanical function relations. Annu Rev Mater Sci 28:271–298